2008-07-15

Investigating and Modeling Possible Mechanisms by Which Healthy Cell Membranes Become Resistant to Hydrolysis by Secretory Phospholipase A2

Jennifer Nelson
Brigham Young University - Provo

INVESTIGATING AND MODELING POSSIBLE MECHANISMS BY WHICH HEALTHY CELL MEMBRANES BECOME RESISTANT TO HYDROLYSIS BY SECRETORY PHOSPHOLIPASE A2

By

Jennifer Nelson

A thesis submitted to the faculty of Brigham Young University

In partial fulfillment of the requirements for the degree of

Master of Science

Department of Physiology & Developmental Biology

Brigham Young University

August 2008

BRIGHAM YOUNG UNIVERSITY

GRADUATE COMMITTEE APPROVAL

Of a thesis submitted by

Jennifer Nelson

This thesis has been ready by each member of the following graduate committee and by majority vote has been found to be satisfactory.

_____	_____
Date	John D. Bell, Chair
_____	_____
Date	Allan M. Judd
_____	_____
Date	William S. Bradshaw

BRIGHAM YOUNG UNIVERSITY

As chair of the candidate's graduate committee, I have read the thesis of Jennifer Nelson in its final form and have found that (1) its format, citations, and bibliographical style are consistent and acceptable and fulfill university and department style requirements; (2) its illustrative materials including figures, tables, and charts are in place; and (3) the final manuscript is satisfactory to the graduate committee and is ready for submission to the university library.

_____ _____

Date

John D. Bell
Chair, Graduate Committee

Accepted for the Department

_____

James P. Porter
Department Chair

Accepted for the College

_____

Rodney J. Brown
Dean, College of Life Sciences

ABSTRACT

INVESTIGATING AND MODELING POSSIBLE MECHANISMS BY WHICH HEALTHY CELL MEMBRANES BECOME RESISTANT TO HYDROLYSIS BY SECRETORY PHOSPHOLIPASE A2

Jennifer Nelson

Department of Physiology and Developmental Biology

Master of Science

Secretory phospholipase A2 (sPLA2) behaves differently toward the membranes of healthy cells compared to those of damaged or dying cells. The enzyme catalyzes rapid and sustained hydrolysis of compromised cells consistent with a simple catalytic mechanism. In contrast, when healthy cells are incubated with sPLA2, they become resistant to hydrolytic attack as manifest by three unusual observations: First, hydrolysis is transient and represents only a small fraction of the total membrane phospholipid content. Second, subsequent

addition of sPLA2 fails to generate additional product. Third, the apparent potency of the enzyme to cause the membrane to be refractory is much greater than the potency for catalyzing hydrolysis. The mechanism responsible for this resistance has not yet been identified. Using Monte Carlo and direct analytical methods, we have developed a model capable of explaining all three of these observations. The model requires two salient elements: only a small pool of phospholipids in the healthy cell membrane is available for catalysis by sPLA2, and hydrolyzed phospholipids are re-acylated and restored very slowly to the accessible pool. The requirement for initial hydrolysis (as opposed to the simple physical presence of the enzyme as previously thought) was confirmed experimentally. Additional evidence has shown that the membrane does not remain permanently in its resistant state. Over time, the membrane resets to its original state. The model also predicts that total substrate, reacylation rate, and the return rate of phospholipids to the membrane should all be constant as enzyme concentration is varied. This prediction was tested by quantitative analysis of hydrolysis time courses at varied enzyme concentrations. Experiments with fluorescent probes, merocyanine 540 and laurdan suggest, that resistance may also involve physical changes to the membrane beyond the kinetic mechanisms hypothesized in the model.

ACKNOWLEDGEMENTS

I gratefully acknowledge my mentor John Bell for his insight in guiding me through this project. My committee members: William Bradshaw and Allan Judd have been instrumental as well. I am grateful to have shared this experience with my two fellow graduate students Rachel Bailey and Erin Olson. Some exceptional undergraduates worked hard to make this project a success. I would in particular like to thank Christa Ellis for her excellent theoretical work in developing the Monte Carlo simulations as well as Celestine Yeung for her hard work in performing and analyzing many experiments. I am also grateful to my sister Rebecca Nelson for putting her proofreading skills to work on my thesis. Finally, I thank my husband Timothy Keller for his loving support.

Table of Contents

Introduction

Secretory phospholipase A2 ($sPLA_2$) belongs to a large family of enzymes that catalyze the hydrolysis of phospholipids. Phospholipases have important physiologic functions, but have also been implicated in many pathophysiologic conditions (Vadas et al., 1993;Murakami et al., 2001). There are many different isoforms that belong to this family of enzymes. Specifically, $sPLA_2$ hydrolyzes the sn-2 acyl bond in a calcium dependent manner and produces free fatty acid and lysophospholipid as products. $sPLA_2$ is one of relatively few enzymes capable of catalyzing its reaction at the interface of the cell membrane and the extracellular fluid. Our laboratory has focused on understanding how $sPLA_2$ interacts with the cell membrane. Ample evidence suggests that the intrinsic properties of the membrane govern whether or not $sPLA_2$ has access to lipid substrate. Catalysis is preceded by two essential steps. First, the enzyme adsorbs to the surface of the cell membrane, and second, substrate migrates from the bilayer into the active site of the enzyme (Figure 1; Gelb et al., 1995; Berg et al., 1997). Regulation of this second step is critical in determining the degree of susceptibly cells exhibit towards $sPLA_2$.

We discovered an intriguing phenomenon: $sPLA_2$ behaves differently toward healthy cell membranes than toward those of damaged or dying cells. The enzyme catalyzes rapid and sustained hydrolysis of compromised cells

consistent with a simple catalytic mechanism (Figure 2, Panel A, dashed curve; Wilson et al., 1999; Gelb et al., 1995; Wilson et al., 1999). In contrast, when healthy cells are incubated with $sPLA_2$, they become resistant to hydrolytic attack as manifest by three unusual observations. First, hydrolysis is transient and represents only a small fraction of the total membrane phospholipid content (Figure 2, Panel A, solid curve; (Wilson et al., 1999). The amount of product decreases due to reacylation of species generated in the reaction. Second, subsequent addition of $sPLA_2$ fails to generate additional product (Figure 2, Panel B; Wilson et al., 1999). Third, the enzyme's apparent potency to cause the membrane to be refractory is much greater than its potency for catalyzing hydrolysis (Figure 2, Panel C). The mechanism responsible for this resistance has not yet been elucidated. The first part of this project focuses on developing a theoretical model capable of explaining resistance, and the second part tests the model experimentally and characterizes the biophysical changes that take place as a cell membrane becomes resistant to hydrolysis.

Materials and Methods

Reagents

Acrylodan-labeled fatty acid-binding protein (ADIFAB), laurdan, and merocyanine 540 (MC540) were obtained from Invitrogen (Carlsbad, CA). Laurdan and MC540 were suspended in dimethylsulfoxide (DMSO). ADIFAB

was suspended in 50 mM KCl and 3 nM NaN_3. Aspartate-49 phospholipase (APPD49 $sPLA_2$) was purified from the venom of *A. p. piscivorus* using the protocol outlined in (Maraganore et al., 1984).

Cell Culture

The cells used in all experiments were S49 mouse lymphoma cells. Cells were maintained in a carefully controlled environment: 37° C, humidified air, and 10% CO_2 (Wilson et al., 1997).

Ca^{2+} and EDTA experiments

Cells were suspended in MBSS that did not contain Ca^{2+}. The reaction progress was monitored using ADIFAB (excitation, 390 nm; emission 432 nm and 505 nm; 65 nM final concentration; (Harris et al., 2002). EDTA, a Ca^{2+} chelator was added at 150 seconds, 20 μL of 0.1 mg/mL of $sPLA_2$ were added at 500 seconds, and 20 μL of 3 nM Ca^{2+} were added at 750 seconds. In the control experiment, the addition order of $sPLA_2$ and Ca^{2+} was reversed to ascertain that the amount added of Ca^{2+} was sufficient to activate $sPLA_2$.

Two Hit Experiments

An aliquot (0.5-4 x 10^6) of cells suspended in MBSS were transferred to a cuvette and placed in the fluorometer (Fluoromax 3, Horiba Jobin-Yvon, Edison, NJ) and maintained at 37° C. At 100 seconds, ADIFAB was added to monitor fatty acid production (Wilson et al., 1997). At 400 seconds, a dose of APPD49

$sPLA_2$ (0.02-70 nM final concentration) was added. At 900 seconds, an additional dose of 20 μL of 0.1 mg/mL APPD49 $sPLA_2$ (70 nM final concentration) was added.

Long Reversal Experiments

An aliquot (0.5-4 x 10^6) of cells suspended in MBSS were transferred to a cuvette and placed in the fluorometer and maintained at 37° C. At 100 seconds, ADIFAB was added to monitor the reaction progress. At 400 seconds, a dose of APPD49 $sPLA_2$ (70 nM final concentration) was added. At 900 seconds, an additional dose of 20 μL of 0.1 mg/mL APPD49 $sPLA_2$ (70 nM final concentration) was added. Cells were then transferred to a centrifuge tube, washed, and resuspended in medium with or without serum and incubated for 0 to 24 hrs. After incubation, cells were again washed, resuspended in MBSS, and transferred to a cuvette, and the same experimental time course was repeated.

Quantification of Experiments Using ADIFAB

Data acquired from the ADIFAB experiments were quantified by calculation of the generalized polarization (GP): $(I_{505} - I_{432})/ (I_{505} + I_{432})$. The GP was then fit using a derived equation designed to model the system under study (see section below).

To determine how much hydrolysis and resistance occurred for a particular dose of $sPLA_2$, the following formulas were used (Figure 3):

Hydrolysis equaled the change in ADIFAB GP from the first dose of $sPLA_2$ (ΔHy) divided by the change in GP from a control dose of 70 nM, a concentration which causes maximum hydrolysis (ΔTo).

$$Hydrolysis = \frac{\Delta Hy}{\Delta To}$$

Resistance equaled the value one subtracted by the change in ADIFAB GP from the second dose of $sPLA_2$ (ΔRe) divided by the change in GP from a control dose of 70 nM (ΔTo).

$$Resistance \quad = 1 - \frac{\Delta \mathrm{Re}}{\Delta To}$$

Cell Growth Curve Experiments

An aliquot (5 mL) of cells which had been suspended to come to full density in 48 hours were treated with 50 μL $sPLA_2$. Control cells received 50 mM KCl and 3 mM NaN_3 (solution in which $sPLA_2$ is suspended in). Every 6 to 12 hours a 100 μL sample was taken from both the control and treatment flasks and gently mixed with 100 μL trypan blue. The number of both viable cells and dead cells was recorded. Data were normalized by dividing all subsequent time points by the initial cell count. Data were plotted and fit using nonlinear regression.

Assessment of Physical Changes that Correspond to Membrane Resistance

Two probes were used to quantify and characterize membrane properties of resistant cells: MC540 (excitation 540 nm, emission wavelengths recorded: 570, 585 nm), which measures interlipid spacing and laurdan (excitation 350 nm, emission wavelengths recorded: 435, 500 nm), which measures invasion of the bilayer surface by water molecules. Experiments were performed using a fluorometer, which permits assessment of global changes.

Cells were harvested, washed, resuspended in 2 mL of MBSS, and incubated with MC540, 170 nM Final, (or laurdan, 50 nM Final) at 37° C in the fluorometer. After equilibrium was reached, a dose of $sPLA_2$ (0.7 nM to 70 nM) was added, and changes in the fluorescence were monitored during a time course of 1800 seconds. The time courses generated were fitted using nonlinear regression. For MC540, these fits allowed for determination of the maximum change in the ratio of intensities observed at 570 and 585 nm as well as the maximum change in the total intensity at 570 and 585 nm. For laurdan, the maximum change in total intensities as well as maximum change in GP were measured.

Theory

Monte Carlo Simulations

The Monte Carlo program consists of a continuous two-dimensional hexagonal array capable of simulating the cell surface. Enzymes can bind to any of the 2000 available sites provided that another enzyme is not bound to an adjacent site (to accommodate steric hindrance). Each binding site consists of 7 phospholipids. The program is capable of varying a large number of parameters (see Table 1), including those in the reaction scheme shown in Figure 4, and can accommodate a second addition of enzyme. The properties of the membrane are adjustable. A proportion of the membrane can be nonhydrolyzable (the enzyme can bind to the site but no catalysis can occur). The affinity of the enzyme can be different for hydrolyzable and nonhydrolyzable sites. The affinity of the enzyme can also be orientation-dependent; i.e. the binding depends on which part of the enzyme surface faces the membrane. There are several ways in which an enzyme can move to a new site on the membrane. In addition to the typical mode of disassociation and readsorption to a new site on the membrane, the enzyme can roll (new orientation) or scoot (same orientation) directly across the surface to a new site. Once the properties of the membrane and enzyme have been set, the program iterates a decision-making routine (Figure 5), and data are generated in the form of a time course. There are two outcomes that are reported at the end of

each cycle: the number of enzymes molecules adsorbed to the membrane and the amount of product.

Analytical Derivation

The distribution of phospholipids among structural states (substrate (S), reaction product (P) and reacylated product (P*)) was modeled by the following system of differential equations:

$$\frac{dP}{dt} = E_B k_{cat}(S_T - P - P^*) - k_{acyl} P \quad (1)$$

$$\frac{dP^*}{dt} = k_{acyl} P - k_r P^* \quad (2)$$

S_T is the total amount of substrate. k_{cat} is the catalysis rate. k_{acyl} is the rate of reacylation. k_r is the rate of return of reacylated lipids to the hydrolyzable pool.

The system assumes rapid equilibrium between the bound and free states of the enzyme and was derived in terms of E_B (the bound state).

$$E_B = \frac{E_T K_{app}}{1 + E_T K_{app}} M_T \quad (3)$$

E_T is the total amount of enzyme. K_{app} is the equilibrium constant for enzyme adsorption and substrate migration. M_T is the total amount of membrane.

Integration of Equation 1 yields Equation 4 with the substitutions listed in Equations 5 and 6.

$$let\ A = E_B k_{cat} S_T$$

$$P = \frac{A}{a-b}\left(e^{-at} - e^{-bt}\right) + \frac{Ak_r}{ab}\left(1 - \frac{b}{b-a}e^{-at} + \frac{a}{b-a}e^{-bt}\right) \quad (4)$$

$$a = \frac{(k_r + A + k_{acyl}) + \sqrt{(k_r + A + k_{acyl})^2 - 4[k_r(A + k_{acyl}) + k_{acyl}A]}}{2} \quad (5)$$

$$b = \frac{(k_r + A + k_{acyl}) - \sqrt{(k_r + A + k_{acyl})^2 - 4[k_r(A + k_{acyl}) + k_{acyl}A]}}{2} \quad (6)$$

To facilitate fitting with nonlinear regression, the data were fit with Equation 7, a simplified version of Equation 4.

$$P = \frac{A}{a-b}\left(e^{-at} - e^{-bt}\right) + \frac{B}{ab}\left(1 - \frac{b}{b-a}e^{-at}\right) + I \quad (7)$$

Theoretical Results

Monte Carlo Simulations

In simulation trials, each parameter was systematically varied to assess its effect on the product time course. If no reacylation occurred, a typical time course looked like Panel A Figure 6. If reacylation occurred but reacylated lipids were available for rehydrolysis, a typical time course looked like Panel B Figure 6. In contrast, if the reacylated substrate was not available for hydrolysis, the shape of the time course changed dramatically, and the shape depended greatly

on the reacylation rate (Panel C Figure 6). Simulated data matched experimental time courses best when the reacylation rate was very small (0.005). When parameters were set to the values indicated in Table 2, the simulated product time course exhibited a form very similar to experimental results (Figure 7).

Fitting Routine

A, *a*, and *b* were constrained based on enzyme concentration and independent assessment of K_{app}.

The value of k_r was allowed to float.

Since the amount of substrate remaining at the time of the second addition of enzyme is unknown, the value of A for the second enzyme addition (A2) was allowed to float.

The model predicted that k_r should vary randomly around a constant value while A2 should decrease with increasing initial dose of enzyme. When applied to actual experimental data, the parameters from the fits behaved as expected (Figure 8). Fits of experimental data for three different enzyme concentrations are shown in Figure 9.

Experimental Results

Resistance is Hydrolysis-Dependent

Incubation of cells while temporarily inhibiting $sPLA_2$ catalysis showed that hydrolysis is required for resistance to occur. In the presence of EDTA, no

catalysis occurred because no free Ca^{2+}, a necessary cofactor, was available. If adsorption of $sPLA_2$ alone were capable of inducing resistance by some biophysical or biochemical means, then subsequent addition of Ca^{2+} would have yielded no hydrolysis. However, when Ca^{2+} was added, hydrolysis occurred (Panel B Figure 10). Positive controls were also included to ascertain that the amount of Ca^{2+} added was sufficient to restore the enzyme to full catalytic activity (Panel A Figure 10). These experiments provided evidence that adsorption of enzyme to the surface of the cell is not enough to cause resistance.

Reversibility of Resistance

After cells had become resistant to the enzyme (exposure to 70 nM final concentration $sPLA_2$), they were washed and resuspended in various solutions (MBSS, medium, and medium plus serum) and incubated at 37° C for different periods of time (0, 1, 6, 12, and 24 hours). After the prescribed incubation time, cells were washed and resuspended in MBSS. Another dose of $sPLA_2$ was added and the amount of hydrolysis was measured. If the cell membrane was still resistant, then minimal or no hydrolysis was expected. If the cell membrane had begun to revert to its state prior to $sPLA_2$ exposure, then an appreciable amount of hydrolysis was expected. Interestingly, the rate at which the membrane reverted to its normal state (condition prior to exposure to $sPLA_2$) depended on what the cells were suspended in. Cells suspended in MBSS showed little or no

reversal (Panel A Figure 11). Cells in culture medium (Panel B Figure 11) with no serum (or with serum, not shown) showed rapid reversal.

Biophysical Changes in the Cellular Membrane

Previous experiments conducted with S49 mouse lymphoma cells revealed pronounced changes in membrane structure that corresponded to increased susceptibility to $sPLA_2$ (Bailey et al., 2007). The order of lipids in the membrane decreased and interlipid spacing increased. Similar experiments were conducted to assess what changes, if any, occurred as the membrane became resistant to hydrolytic attack.

Lipid Order in the Resistant Cell Membrane

Addition of $sPLA_2$ to the cell suspension caused a rapid decrease in apparent lipid order, as assessed by laurdan GP (Figure 12). Repetition of the experiment at various $sPLA_2$ concentrations demonstrated that the effect was saturable and reproducible. The maximum change was 0.02 ± 0.01 GP units with an EC_{50} value of 5.79 ± 3.48 nM $sPLA_2$ (blue curve, Figure 12). The total intensity of laurdan also decreased with increasing concentration of $sPLA_2$ (maximum change of 5% decrease, pink curve, Figure 12) with an EC_{50} value of 0.23 ± 0.005.

Lipid Spacing in the Resistant Cell Membrane

Interlipid spacing also changed as the membrane became resistant to hydrolysis. The dose dependent decrease in total MC540 intensity with

increasing concentration of $sPLA_2$ (maximum decrease of 12%, EC_{50} 0.71 ± 0.43) indicated that the lipids in the cell membrane became more tightly packed (Figure 13).

Effect of sPLA2 on Cell Growth

Over an incubation period of 48 hours with 70 nM dose of $sPLA_2$, cell growth appeared to be unaffected by the presence of enzyme. The doubling time for the control cells was 10.32 ± 0.10 hours and 13.27 ± 0.37 hours for the cells incubated with $sPLA_2$ (Figure 14).

Discussion

It is simple to establish that cell membranes become resistant to $sPLA_2$ (Wilson et al., 1999); however, the mechanism governing resistance needs to be better understood. Two plausible hypotheses are easily excluded. The first centers on the idea of rapid endocytosis of $sPLA_2$. Sequestration of the enzyme inside the cell would prevent hydrolysis of the outer-leaflet; however, three pieces of evidence refute this idea. First, a membrane that has become resistant to hydrolysis can rapidly be rendered susceptible by the addition of ionomycin, a calcium ionophore (Bailey et al., 2007). Thus, if the enzyme were sequestered, it is unlikely that it would be regurgitated on the time scale of the experiment. Second, flow cytometry data reveal that only a small percentage of the $sPLA_2$ is endocytosed; a large proportion is still present extracellularly and presumably

capable of carrying out catalysis (Bailey et al., 2007). Third, a second maximum dose of enzyme (70 nM final concentration) elicits no hydrolysis. It is difficult to imagine a situation in which the cell could completely sequester the second dose of enzyme before any hydrolysis occurred since it was unable to do so with the first.

The second possible explanation for resistance centers on a receptor-mediated response to the presence of $sPLA_2$. However, two pieces of evidence suggest that this is not the case. First, if resistance depended on $sPLA_2$ binding to a receptor, then enzymes which do not bind to the receptor would be incapable of causing resistance. However, experiments done by Wilson et al. (1999) showed that bee venom $sPLA_2$, which does not bind to $sPLA_2$ receptor (M-type, Ancian et al., 1995), can cause resistance. Second, our experiments indicate that hydrolysis is required for resistance to occur. When cells were incubated in Ca^{2+}-free MBSS with $sPLA_2$, the presence of the enzyme on the cell surface did not trigger resistance. It was only after Ca^{2+} had been added back into solution and $sPLA_2$ became active that resistance occurred. These two observations argue that the resistance is not a receptor-mediated response.

The next general hypothesis is whether resistance can be explained entirely by the interactions of $sPLA_2$ with the membrane. When we simulated the interactions between $sPLA_2$ and the cell membrane using a Monte Carlo

algorithm, we identified what could potentially be the most important variables. From the many simulations performed, two critical conclusions emerged. First, the hydrolysis reaction must slow significantly or come to a complete stop. The easiest way to satisfy this criterion is to limit the amount of substrate available to the enzyme. Exhaustion of this pool would explain why the cell membrane has become resistant. Second, the rate at which reacylated lipids are returned to the available substrate pool must be much smaller than the rate of reincorporation of fatty acid into phospholipids. When these two conclusions are in force, the results of simulated time courses closely resemble experimental time courses (Figure 15). To restate, the minimum model for resistance centers on a small, rapidly hydrolyzable pool of lipids that upon exhaustion is slowly repopulated over time.

A system of differential equations based on this minimum model (limited substrate hypothesis) is capable of fitting experimental data even when parameters are highly constrained by values determined from independent experimental results. Parameters that were allowed to float behaved as predicted, providing further evidence that the model could correctly provide a mechanism for resistance.

Previous experiments published in Wilson et. al. (1999) showed that resistance occurs even when little or no initial hydrolysis is observed

(experiments used weakly active human group IIA and venom Lys-49). However, due to the high concentrations used in those experiments, the resistance observed could be the result of competition for binding. If the catalytically weak enzymes saturate the surface of the cells, then highly active Asp-49 venom $sPLA_2$ would have diminished access to the membrane. Additionally, these isoforms are incapable of inducing complete resistance (Wilson et al., 1999).

Two lines of evidence suggest that resistance could be more complex than previously thought. The first refers to the rate at which the initial naïve state of the membrane can be restored following exposure to $sPLA_2$. If the limited substrate model applied, one would expect that the reversal of resistance would involve restoration of the original pool of membrane phospholipids and that the timing of the restoration would be fixed based on cellular metabolic processes. Instead, the reversal rate of resistance depended on the solution in which cells were suspended. Since the reversal rate was dependent on the type of cell suspension, a different mechanism could be responsible for the reestablishment of original membrane conditions.

The second reason for believing that resistance is more complex than the limited-substrate model is that fluorescent probes detected changes in the membrane when cells were incubated $sPLA_2$. If these changes were reflective of

resistance, they would be small, logical with respect to susceptibility, and dependent on $sPLA_2$ dose in the appropriate range. As predicted, the observed changes in membrane order (0.02 GP units and 5% maximum drop in normalized total laurdan intensity) and interlipid spacing (12% maximum drop in normalized MC540 intensity) were small (Figures 12 and 13). Moreover, these changes were logical. As cell membranes become susceptible, lipid order decreases and interlipid spacing increases which improves the ability of phospholipids to migrate into the enzyme's active site (Bailey et al., 2007). In contrast, the opposite occurred as resistance emerged; cell membranes became more ordered and interlipid spacing decreased (Figures 12 and 13).

An intriguing observation was the difference in $sPLA_2$ potency for inducing resistance (EC_{50} = 0.49) and catalyzing hydrolysis (EC_{50} = 3.39, Panel C Figure 2). Although the limited-substrate model can reconcile at least a small difference in potency (Figure 16), a more compelling explanation relates to the fluorescence observations. The potencies of the change in total laurdan intensity (EC_{50} = 0.23) and total MC540 intensity (EC_{50} = 0.79) were very similar to the EC_{50} of resistance (0.49). Thus, since the fluorescence changes occurred at the same range of $sPLA_2$ dose as resistance, it is reasonable to conclude that the observed changes in interlipid spacing correspond to resistance. Interestingly, the EC_{50} of laurdan GP (5.79) was very similar to the EC_{50} of hydrolysis (3.39). This result

suggests that the changes in lipid order are more closely linked to hydrolysis. Taken together, the results encourage a hypothesis that products of hydrolysis either directly or indirectly alter membrane structure in a way that makes it resistant to the action of $sPLA_2$.

How might the dose of $sPLA_2$ be different for inducing resistance than for hydrolysis since resistance appears to depend on the enzyme's catalytic activity? When a relatively small amount of available substrate has been hydrolyzed, the reaction products generated in the membrane could be sufficient to alter the domains where productive catalysis can occur, making subsequent hydrolysis less favorable. For this explanation to work, the rate of domain alteration must be slower than the rate of hydrolysis. If the rate of hydrolysis and domain alteration equaled each other, there would be no transient burst of hydrolysis.

Conclusion

The cell membrane is a dynamic environment. The results of this study show the delicate balance between two competing needs: first, the need to generate product that will be used in synthesis of inflammatory molecules in a physiological setting, and second, the need to preserve membrane integrity. Studying how membranes become resistant to $sPLA_2$ reveals the importance of lipid organization in the bilayer. In this case, the properties of the membrane, not

the enzyme, regulate the reaction. Based on the experiments performed in this study, we conclude the following:

Monte Carlo simulations can adequately simulate the interaction of $sPLA_2$ with the cell membrane and indicate the minimum requirements for the resistance phenomenon.

Hydrolysis is required experimentally for resistance to occur.

Tests of the Limited Substrate Model have shown that it is capable of explaining resistance.

Resistance is a reversible phenomenon.

Changes in total MC540 and laurdan fluorescence intensity suggest resistance may involve physical changes in the membrane that interfere with hydrolysis and limit the available substrate pool.

The reversibility of resistance and the physical changes in the membrane that occur during the onset of resistance suggest that resistance may be more complex than previously thought.

References

1. Ancian, P., G. Lambeau, and M. Lazdunski. 1995. Multifunctional activity of the extracellular domain of the M-type (180 kDa) membrane receptor for secretory phospholipases A2. *Biochemistry* 34:13146-13151.

2. Bailey, R. W., E. D. Olson, M. P. Vu, T. J. Brueseke, L. Robertson, R. E. Christensen, K. H. Parker, A. M. Judd, and J. D. Bell. 2007. Relationship between Membrane Physical Properties and Secretory Phospholipase A2 Hydrolysis Kinetics in S49 Cells during Ionophore-Induced Apoptosis. *Biophys. J.* 93:2350-2362.

3. Berg, O. G., J. Rogers, B. Z. Yu, J. Yao, L. S. Romsted, and M. K. Jain. 1997. Thermodynamic and kinetic basis of interfacial activation: resolution of binding and allosteric effects on pancreatic phospholipase A2 at zwitterionic interfaces. *Biochemistry* 36:14512-14530.

4. Gelb, M. H., M. K. Jain, A. M. Hanel, and O. G. Berg. 1995. Interfacial enzymology of glycerolipid hydrolases: lessons from secreted phospholipases A2. *Annu. Rev. Biochem.* 64:653-688.

5. Harris, F. M., K. B. Best, and J. D. Bell. 2002. Use of laurdan fluorescence intensity and polarization to distinguish between changes in membrane fluidity and phospholipid order. *Biochim. Biophys. Acta* 1565:123-128.

6. Maraganore, J. M., G. Merutka, W. Cho, W. Welches, F. J. Kezdy, and R. L. Heinrikson. 1984. A new class of phospholipases A2 with lysine in place of aspartate 49. Functional consequences for calcium and substrate binding. *J. Biol. Chem.* 259:13839-13843.

7. Murakami, M., R. S. Koduri, A. Enomoto, S. Shimbara, M. Seki, K. Yoshihara, A. Singer, E. Valentin, F. Ghomashchi, G. Lambeau, M. H. Gelb, and I. Kudo. 2001. Distinct arachidonate-releasing functions of mammalian secreted phospholipase A2s in human embryonic kidney 293 and rat mastocytoma RBL-2H3 cells through heparan sulfate shuttling and external plasma membrane mechanisms. *J. Biol. Chem.* 276:10083-10096.

8. Vadas, P., J. Browning, J. Edelson, and W. Pruzanski. 1993. Extracellular phospholipase A2 expression and inflammation: the relationship with associated disease states. *J. Lipid Mediat.* 8:1-30.

9. Wilson, H. A., W. Huang, J. B. Waldrip, A. M. Judd, L. P. Vernon, and J. D. Bell. 1997. Mechanisms by which thionin induces susceptibility of S49 cell membranes to extracellular phospholipase A2. *Biochim. Biophys. Acta* 1349:142-156.

10. Wilson, H. A., J. B. Waldrip, K. H. Nielson, A. M. Judd, S. K. Han, W. Cho, P. J. Sims, and J. D. Bell. 1999. Mechanisms by which elevated intracellular calcium induces S49 cell membranes to become susceptible to the action of secretory phospholipase A2. *J. Biol. Chem.* 274:11494-11504.

Tables

Table 1: Monte Carlo Parameters

K_1 = rate of enzyme binding
K_2 = enzyme disassociation rate
K_e = probability that the lipid makes it into the enzyme active site
K_i = rate of inhibition on hydrolysis of occupied, non-hydrolysable sites.
K_{acyl} = rate of reacylation
Orientation effect = binding strength is altered by some factor if the enzyme active-site is down.
non hydrolysable sites = establishes x/2000 sites are unavailable for hydrolysis
Ratio of affinity for non-hydrolysable sites = enzyme affinity for non-hydrolysable sites can multiplied by some factor
T = length of experiment
Initial enzyme concentration
Determines how much additional enzyme will be added at a time point When will the additional enzyme be added?
Reacylation dependent on binding = the reacylation rate can increase every time an enzyme binds to a lipid
Reacylation dependent on hydrolysis = reacylation rate can increase every time a lipid is hydrolyzed.
Reacylated lipids may become unavailable for hydrolysis once they have been reacylated, they become labeled as non-hydrolysable sites.

Table 2: Parameters Values Used to Generate Figure 19A

Parameter	Value
K_1	0.5
K_2	0.5
k_e	0.5
k_{acyl}	0.005
Experiment length	2500
Initial dose of enzyme	50 to 600
Second dose of enzyme	600
Time of second dose addition	1750
Lipids available for rehydrolysis	No

Figures

Figure Legends

Figure 1: Reaction Scheme of sPLA2 with a Membrane E: $sPLA_2$, EB: $sPLA_2$ adsorbed to membrane surface, S: substrate, E_B^S: $sPLA_2$ absorbed to membrane and with substrate bound in the active site, P: hydrolysis product (lysophospholipid and fatty acid), K_1: equilibrium constant for adsorption, K_2: equilibrium constant for substrate migration, k_{cat}: rate of catalysis.

Figure 2: Panel A S49 cells were incubated with 5 uL of ionomycin or DMSO, 20 μL of sPLA2 was added, and the amount of reaction product generated was measured over time using ADIFAB. **Panel B** This figure shows the result of a typical "two hit" experiment. At the gray arrow 20 μL of sPLA2 was added. After a new baseline had been established, a second 20 μL dose of sPLA2 was added as indicated by the black arrow. **Panel C** Analysis of a series of "two hit" experiments. The results of the analysis were fit using non-linear regression. The dashed curve is the resistant curve and the solid curve is the hydrolysis curve.

Figure 3: Method Used to Calculate Resistance and Total Hydrolysis Hydrolysis equaled the change in ADIFAB GP from the first dose of sPLA2 (ΔHy) divided by the change in GP from a control dose of 70 nM, a concentration which causes maximum hydrolysis (ΔTo). Resistance equaled the value one subtracted by the change in ADIFAB GP from the second dose of sPLA2 (ΔRe) divided by the change in GP from a control dose of 70 nM (ΔTo).

Figure 4: Expanded Reaction Scheme of sPLA2 with a Membrane E: sPLA2, EB: $sPLA_2$ adsorbed to membrane surface, S: substrate, E_B^S: $sPLA_2$ absorbed to membrane and with substrate bound in active the site, P: hydrolysis product (lysophospholipid and fatty acid), K_1: equilibrium constant for adsorption, K_2: equilibrium constant for substrate migration, k_{cat}: rate of catalysis, k_{acyl}: rate of reacylation, k_r: rate of return of reacylated lipids to the membrane.

Figure 5: Flow Chart of the Algorithm Executed by the Monte Carlo Simulation

Figure 6: Simulated Time Courses: Panel A Example of a typical time course when the reacylation rate (k_{acyl}) is set to zero. **Panel B** Example of a typical time course when the reacylation is a small number (0.005) and lipids are available for

rehydrolysis. **Panel C** Example of a typical time course when reacylation is a small number (0.005) and lipids are not available for rehydrolysis.

Figure 7: Simulated Time Course: Variation of Initial Enzyme Dose Initial enzyme concentration varied between 50 and 600, kacyl equaled 0.005, and lipids were not available for rehydrolysis.

Figure 8: Results of Fitting Double Dose Experiments with Equation 7 Green curve: parameters A2 (reflects amount of substrate left at time of second addition of enzyme) and purple curve: k_r (reflects reacylation rate).

Figure 9: Examples of Fitting "Two Hit" Experiments with Equation 7 *A*, *a*, and *b* were constrained based on enzyme concentration and independent assessment of K_{app}. The value of k_r was allowed to float. Since the amount of substrate remaining at the time of the second addition of enzyme is unknown, the value of A for the second enzyme addition (A2) was allowed to float. Fits for three different experiments are shown (70.0 nM, 0.2 nM, 0.7 nM).

Figure 10: Results of Ca^{2+} and EDTA experiments Cells were suspended in MBSS that did not contain Ca^{2+}. **Panel A** EDTA was added at 150 seconds, 20 μL of 3 nM Ca^{2+} was added at 500 seconds, and 20 μL of 0.1 mg/mL of $sPLA_2$ was added 750 seconds. **Panel B** EDTA was added at 150 seconds, 20 μL of 0.1 mg/mL of sPLA2 was added at 500 seconds, and 20 μL of 3 nM Ca^{2+} were added at 750 seconds.

Figure 11: Reversal of Resistance: Cells Incubated in MBSS and Medium Panel A Amount of initial hydrolysis (black curve), amount of hydrolysis after incubation 15 minute incubation in MBSS (purple curve). **Panel B** Amount of initial hydrolysis (as measured by change in ADIFAB GP, black curve), amount of hydrolysis after incubation in medium (as measured by change in ADIFAB GP, purple curve).

Figure 12: Change of Laurdan Fluorescent Intensity and GP as a Function of SPLA2 Concentration Cells were suspended in MBSS. After equilibrium was reached, a dose of sPLA2 (0.7 nm to 70 nM) was added and changes in the laurdan fluorescence were monitored during a time course of 1800 seconds. The maximum change in the intensities (blue curve) and GP (pink curve) were calculated.

Figure 13: Change of MC540 Fluorescent Intensity Cells were suspended in MBSS. After equilibrium of the probe was reached, a dose of sPLA2 (0.7 nm to 70 nM) was added and changes in the fluorescence were monitored during a time

course of 1800 seconds. The maximum change in MC540 total intensity (blue curve) was calculated.

Figure 14: Cell Growth is Not Affected by sPLA$_2$ The growth of cells was with and without sPLA$_2$. The growth of control cells is reported in the black curve and the growth of cells treated with 70nM (final concentration) sPLA$_2$ is reported in the green curve.

Figure 15: Comparison of Simulated Double Dose Experiments to Actual Double Dose Experiments Panel A Results of Monte Carlo simulations in which the initial dose of enzyme was varied (50 to 600). The second dose of enzyme (600) was added at 1750. **Panel B** Results of actual double dose experiments in which the initial dose of enzyme was varied (0.02 to 70 nM). The second dose of enzyme (70 nM) was added at 600 seconds.

Figure 16: Comparison of Potencies Generated from Simulated "Two Hit" Experiments The amount of resistance and hydrolysis caused by a particular dose of sPLA2 in the simulated experiments from Panel B Figure 15 was calculated using the method described in Figure 3. The results of the analysis were fit using non-linear regression. The green curve is the resistant curve and the black curve is the hydrolysis curve.

Figure 1

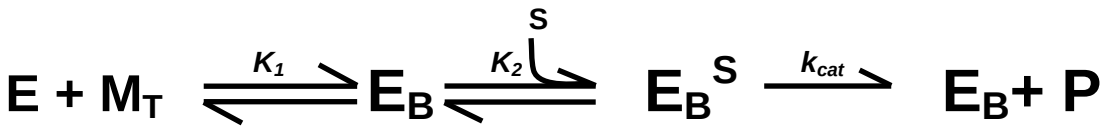

Figure 2

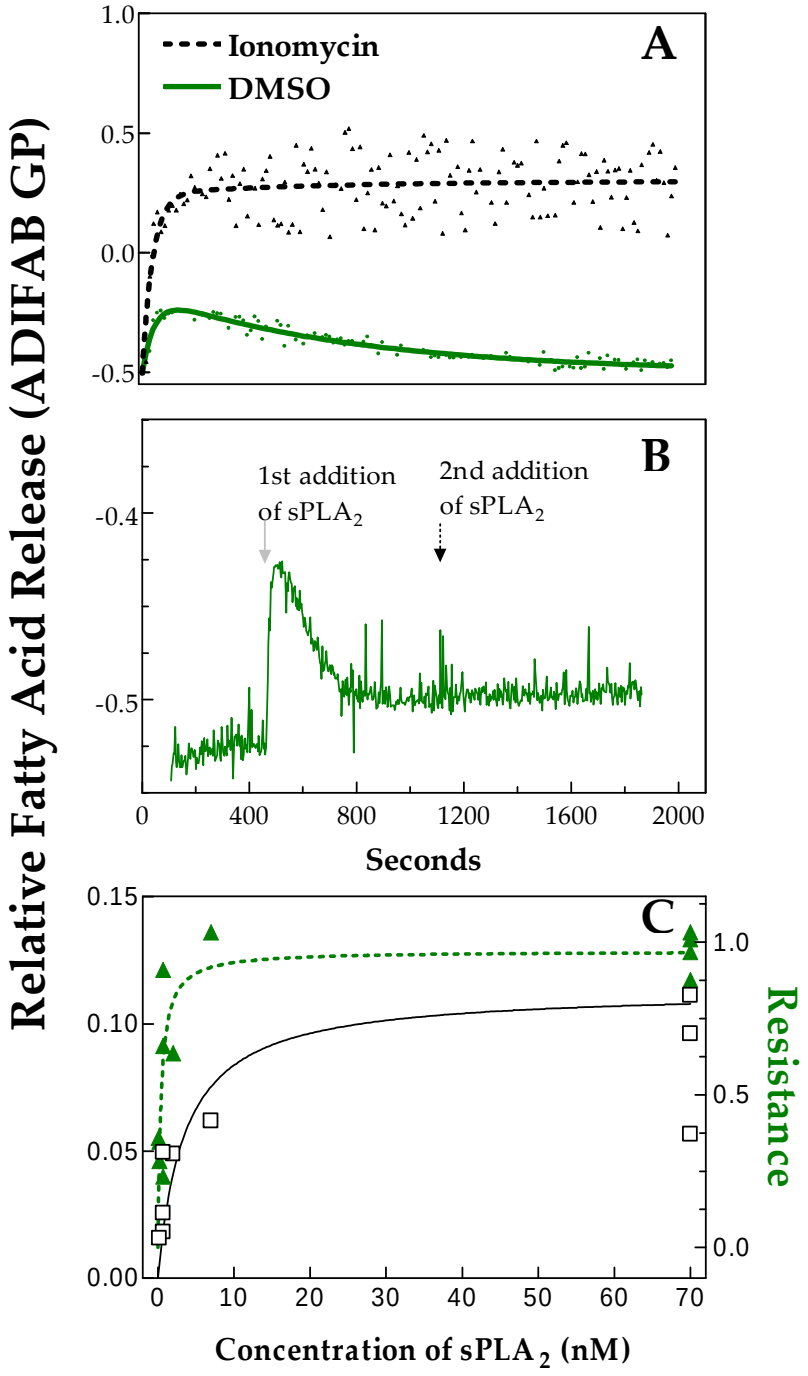
Relative Fatty Acid Release (ADIFAB GP)
Ionomycin
DMSO
A
1.0
0.5
0.0
-0.5
B
1st addition of sPLA2
2nd addition of sPLA2
-0.4
-0.5
0
400
800
1200
1600
2000
Seconds
C
0.15
0.10
0.05
0.00
1.0
0.5
0.0
Resistance
0
10
20
30
40
50
60
70
Concentration of sPLA 2 (nM)

Figure 3

$$Hydrolysis = \frac{\Delta Hy}{\Delta To}$$

$$Resistance \quad = 1 - \frac{\Delta \mathrm{Re}}{\Delta To}$$

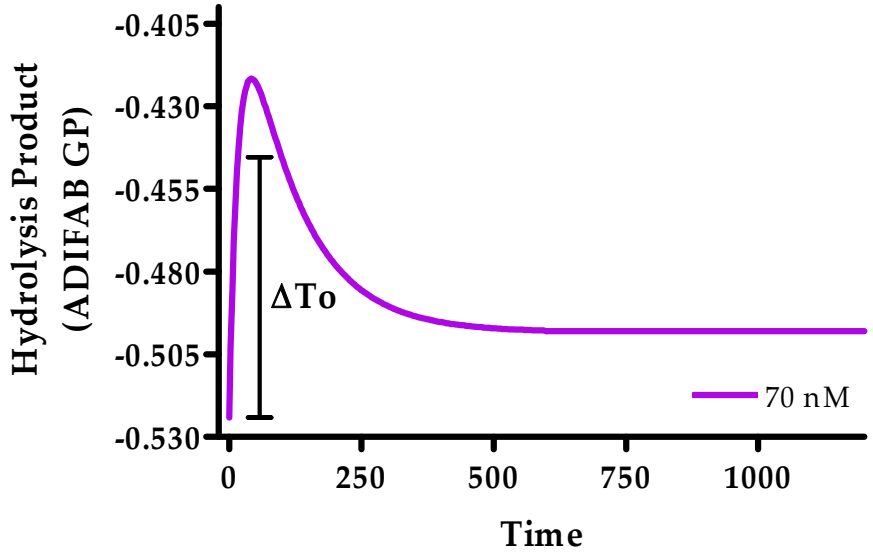

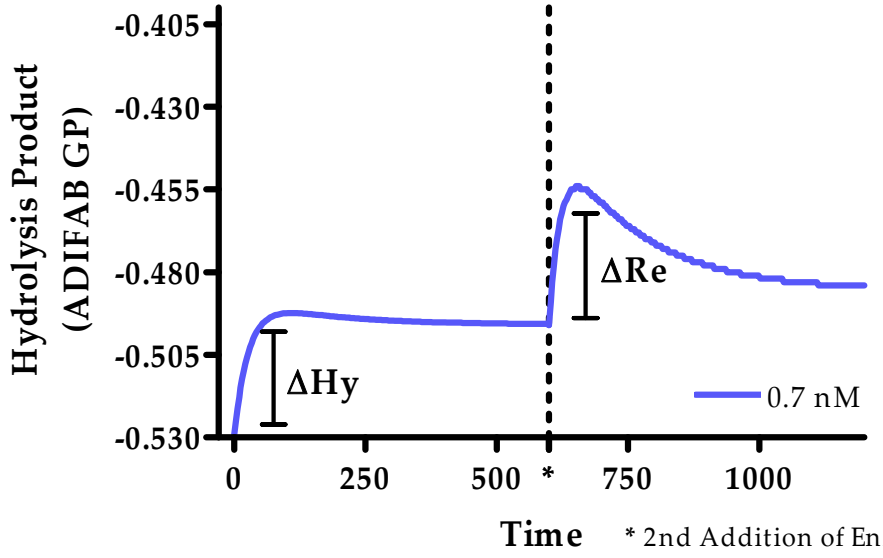

* 2nd Addition of Enzyme 70 nM

Figure 4

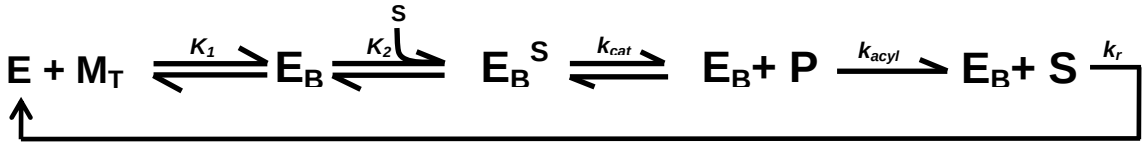

Figure 5

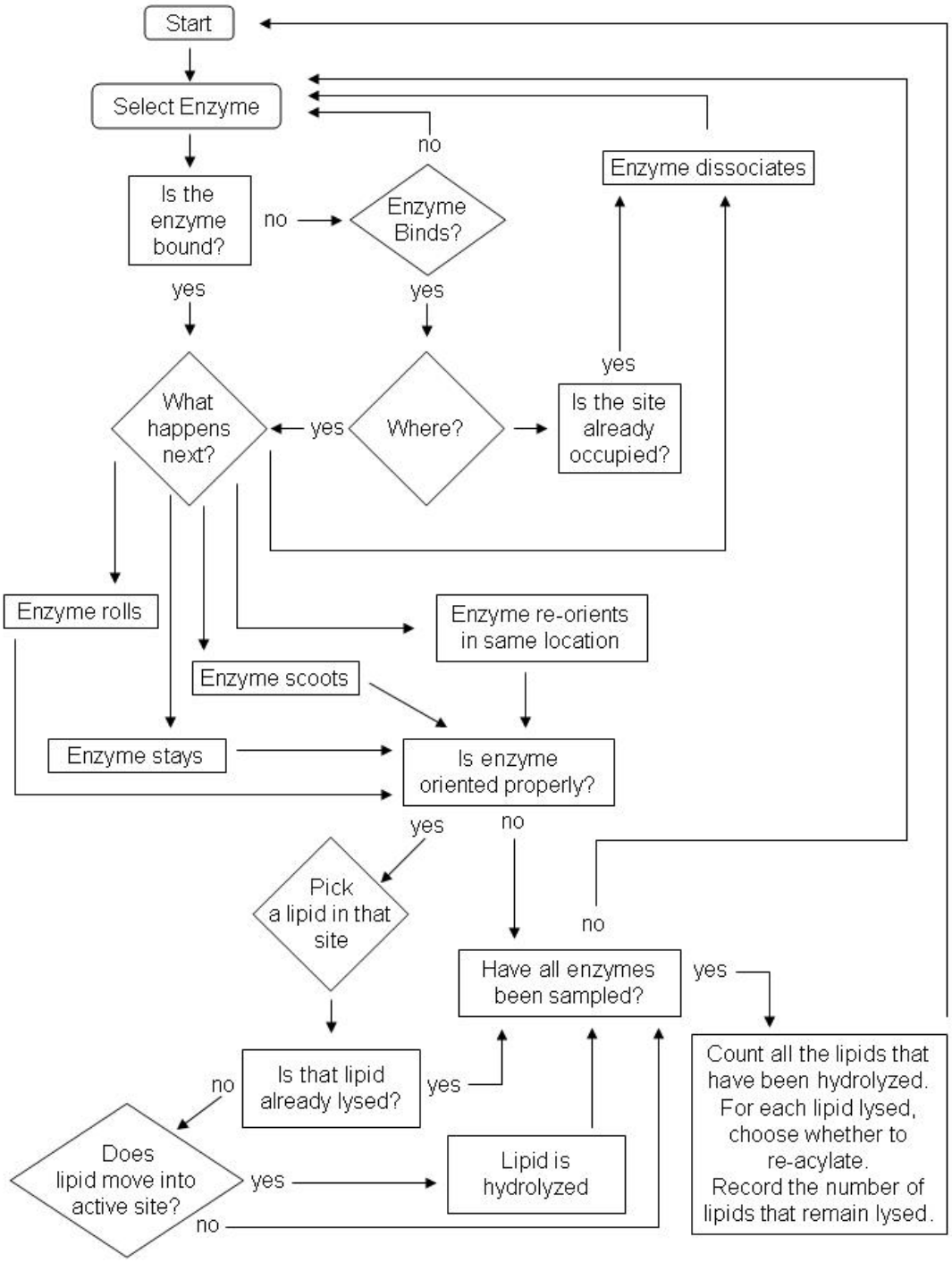
Start
Select Enzyme
Is the enzyme bound?
no
Enzyme Binds?
no
Enzyme dissociates
yes
yes
yes
What happens next?
yes
Where?
Is the site already occupied?
Enzyme rolls
Enzyme re-orients in same location
Enzyme scoots
Enzyme stays
Is enzyme oriented properly?
yes
no
Pick a lipid in that site
no
Have all enzymes been sampled?
yes
Count all the lipids that have been hydrolyzed. For each lipid lysed, choose whether to re-acylate. Record the number of lipids that remain lysed.
Is that lipid already lysed?
no
yes
Does lipid move into active site?
yes
Lipid is hydrolyzed
no

Figure 6

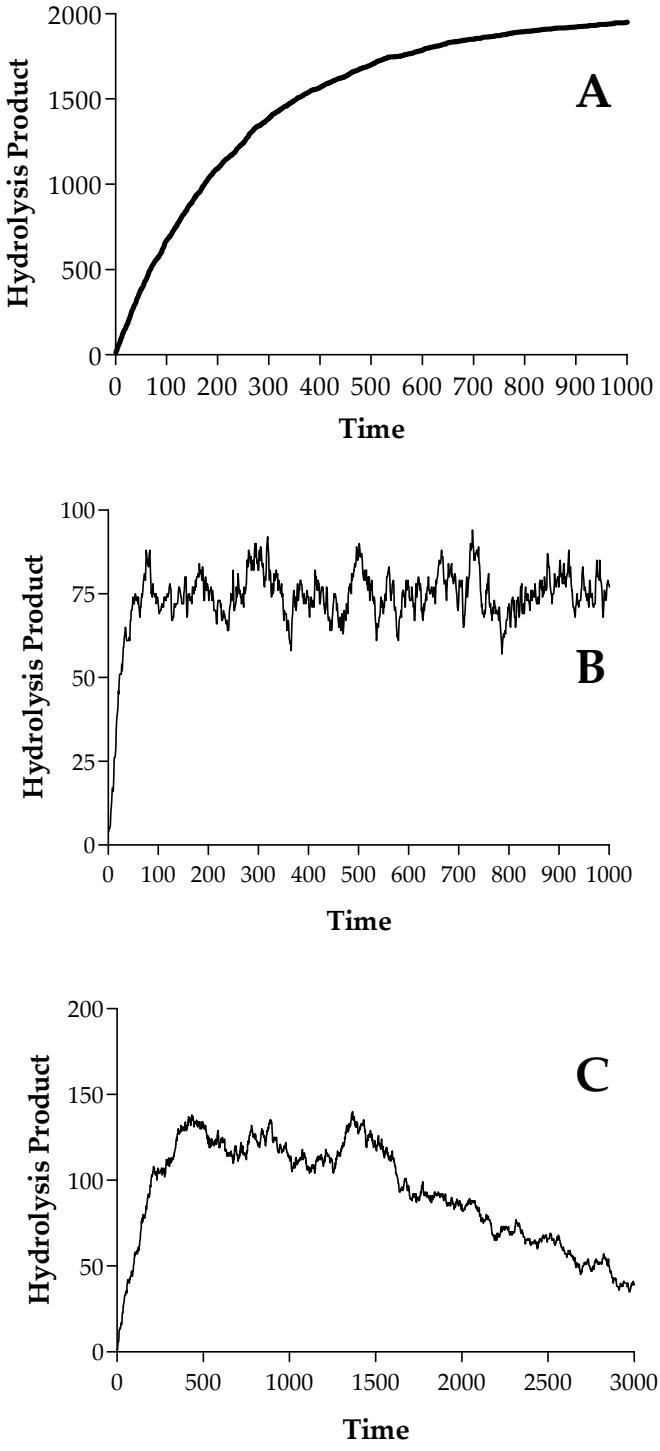
Hydrolysis Product
2000
1500
1000
500
0
0 100 200 300 400 500 600 700 800 900 1000
Time
A
Hydrolysis Product
100
75
50
25
0
0 100 200 300 400 500 600 700 800 900 1000
Time
B
Hydrolysis Product
200
150
100
50
0
0 500 1000 1500 2000 2500 3000
Time
C

Figure 7

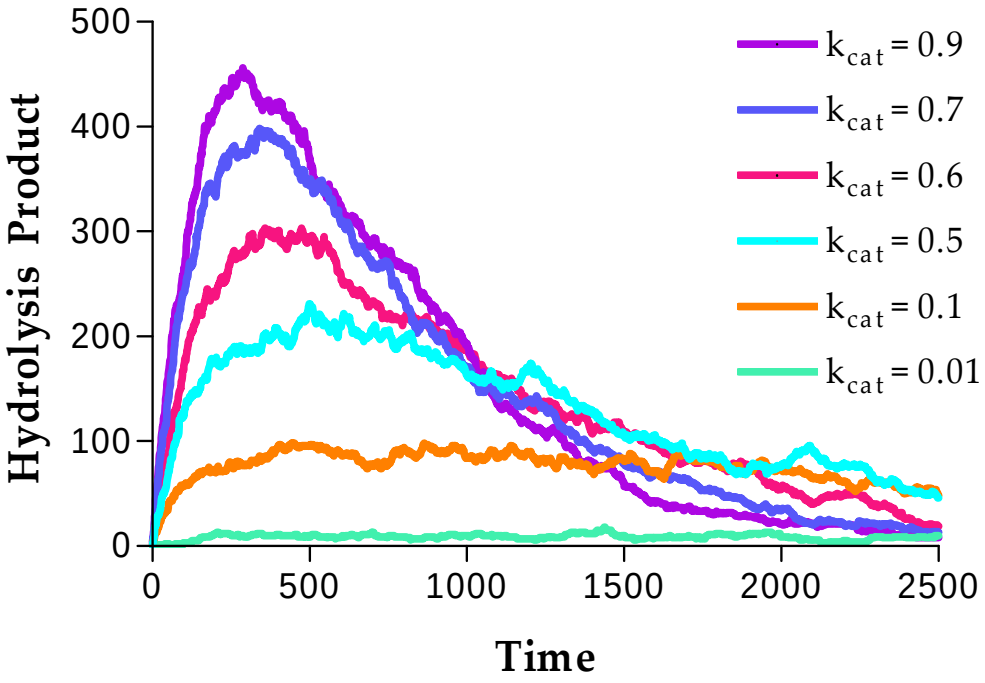
Hydrolysis Product
500
400
300
200
100
0
0
500
1000
1500
2000
2500
Time
k_{cat} = 0.9
k_{cat} = 0.7
k_{cat} = 0.6
k_{cat} = 0.5
k_{cat} = 0.1
k_{cat} = 0.01

Figure 8

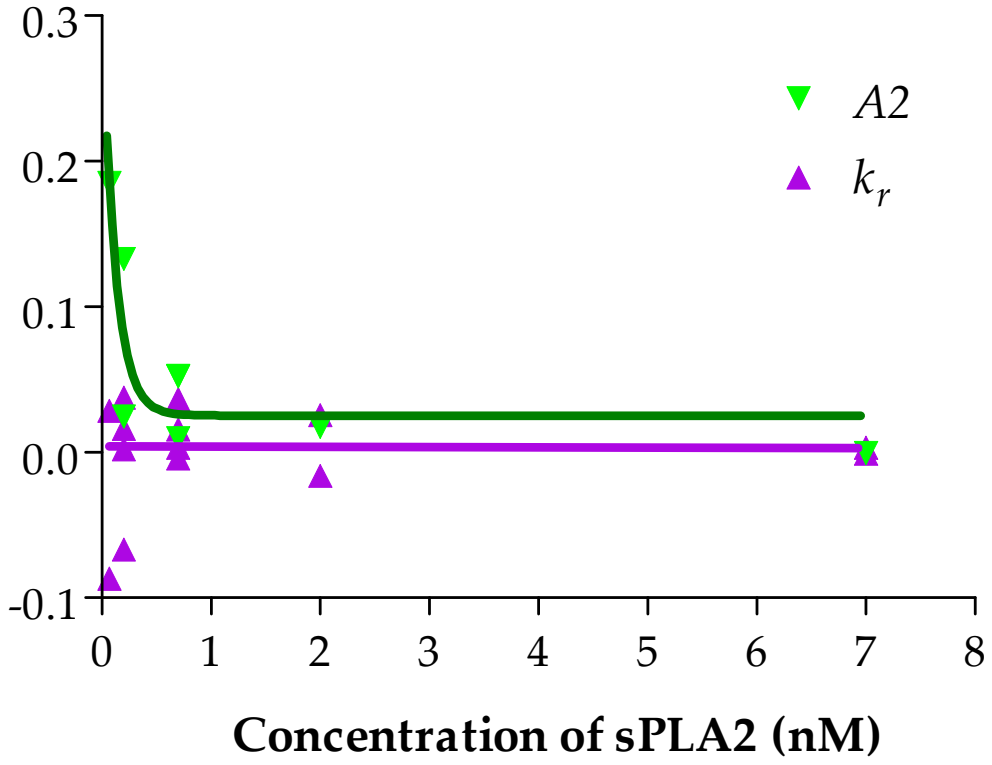

Figure 9

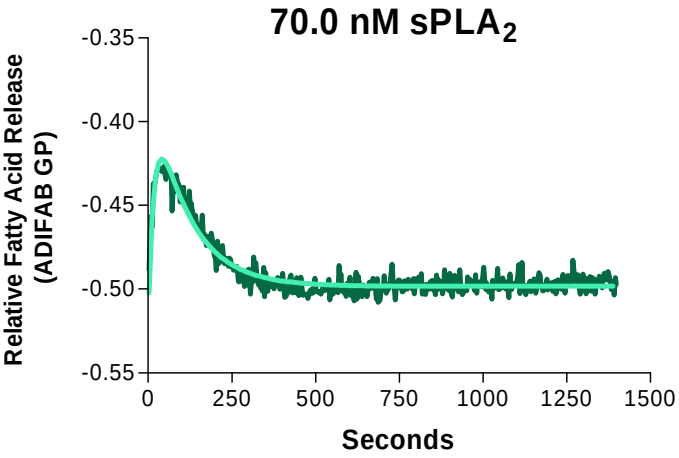
70.0 nM sPLA2
Relative Fatty Acid Release (ADIFAB GP)
-0.35
-0.40
-0.45
-0.50
-0.55
0
250
500
750
1000
1250
1500
Seconds

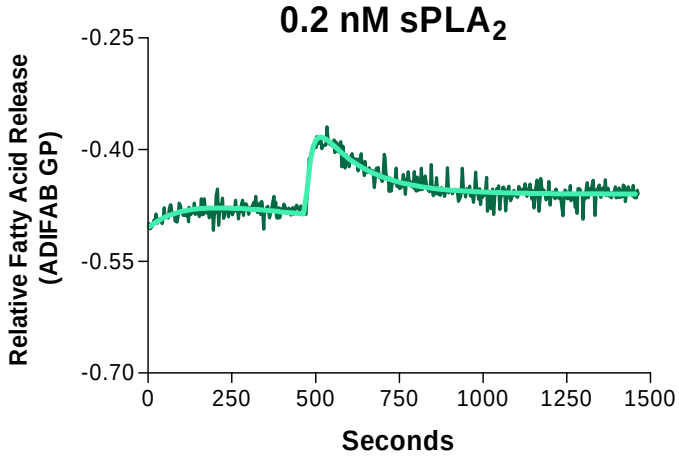
0.2 nM sPLA2
Relative Fatty Acid Release (ADIFAB GP)
-0.25
-0.40
-0.55
-0.70
0
250
500
750
1000
1250
1500
Seconds

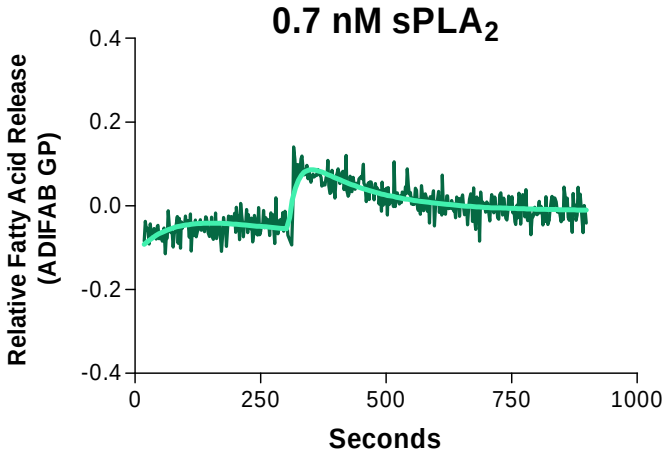
0.7 nM sPLA2
Relative Fatty Acid Release (ADIFAB GP)
0.4
0.2
0.0
-0.2
-0.4
0
250
500
750
1000
Seconds

Figure 10

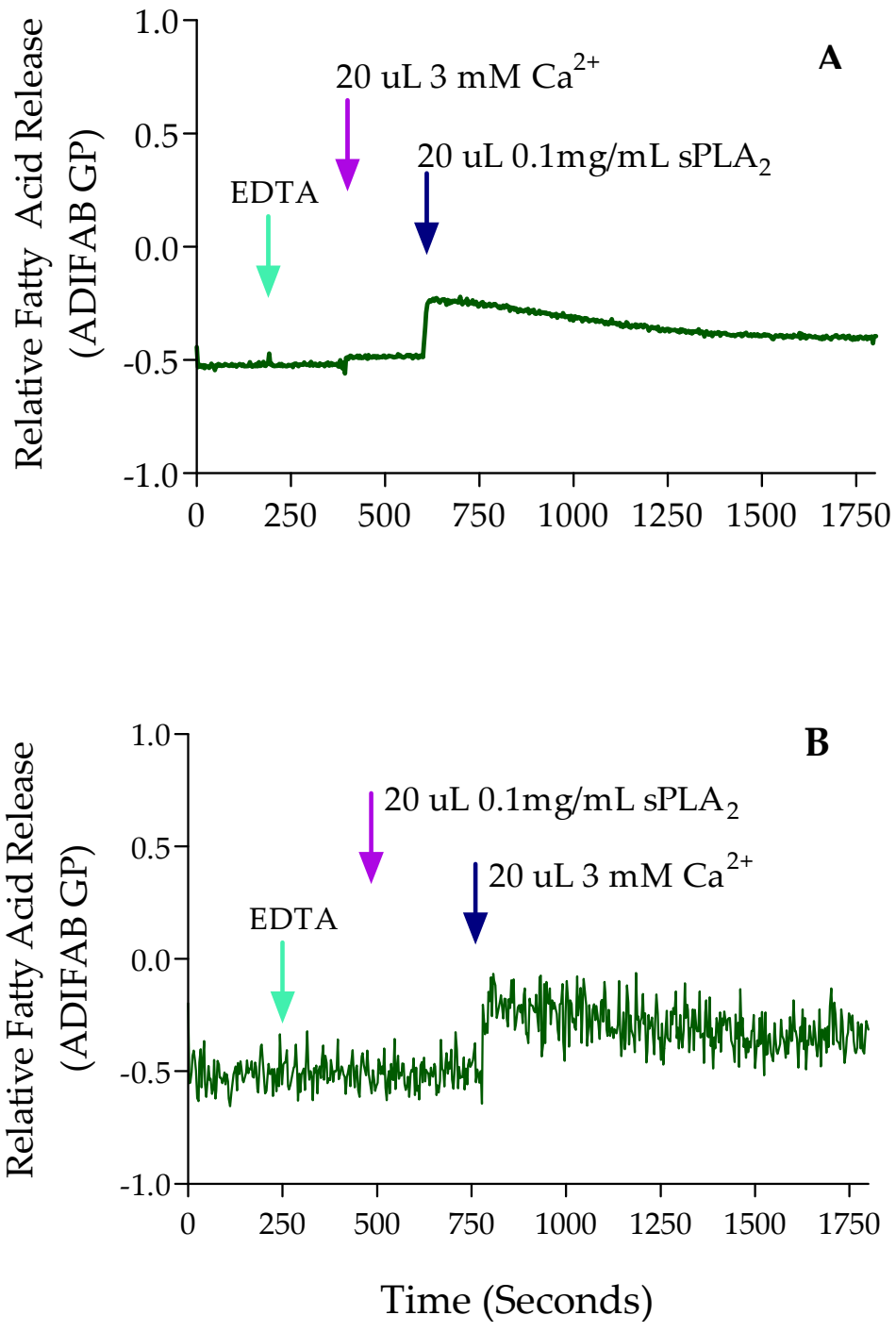
A
20 uL 3 mM Ca2+
20 uL 0.1mg/mL sPLA2
EDTA
Relative Fatty Acid Release
(ADIFAB GP)
1.0
0.5
0.0
-0.5
-1.0
0
250
500
750
1000
1250
1500
1750
B
20 uL 0.1mg/mL sPLA2
20 uL 3 mM Ca2+
EDTA
Relative Fatty Acid Release
(ADIFAB GP)
Time (Seconds)

Figure 11

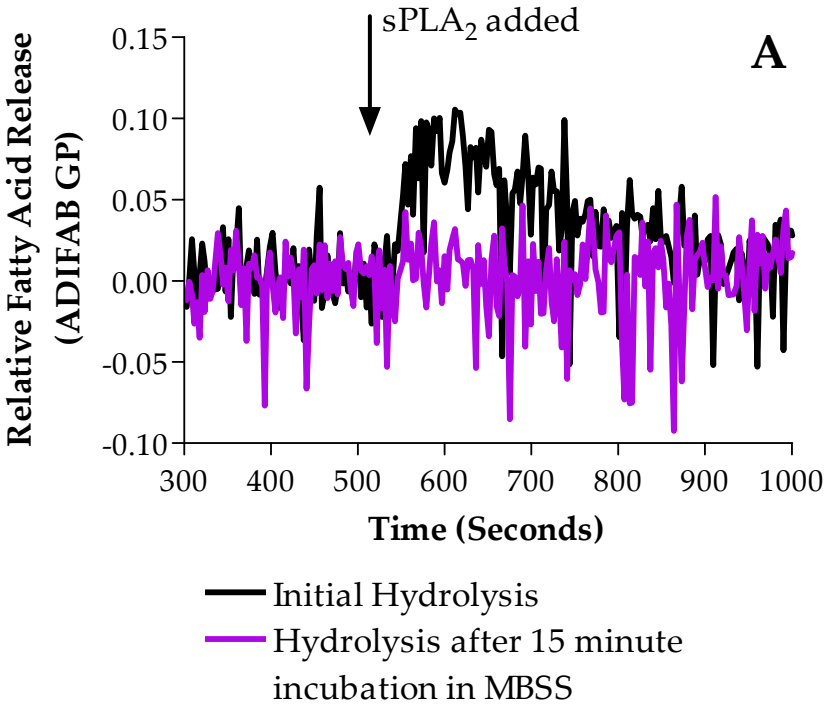
sPLA2 added
A
Relative Fatty Acid Release
(ADIFAB GP)
0.15
0.10
0.05
0.00
-0.05
-0.10
300
400
500
600
700
800
900
1000
Time (Seconds)
Initial Hydrolysis
Hydrolysis after 15 minute incubation in MBSS

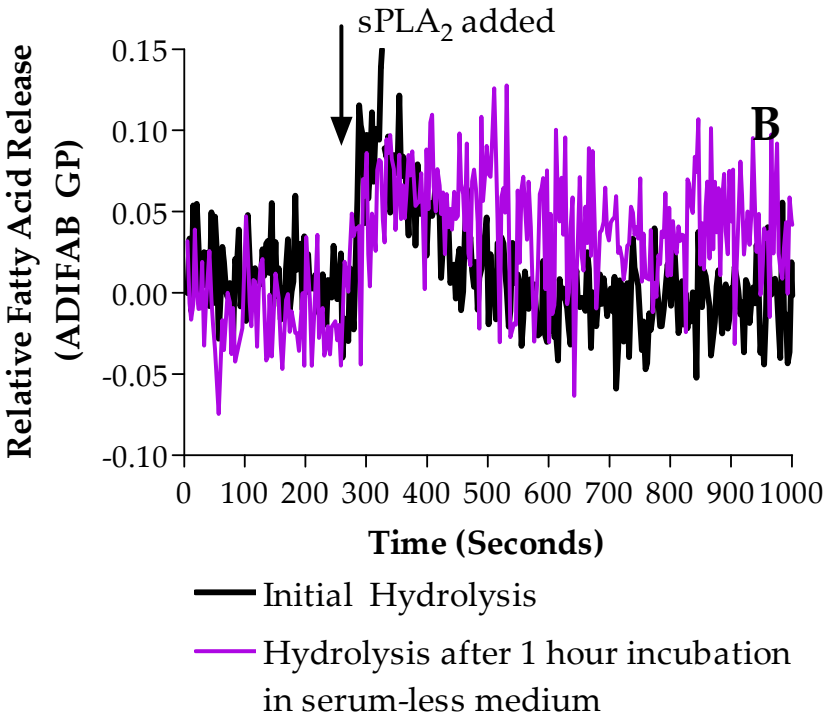
sPLA2 added
B
Relative Fatty Acid Release
(ADIFAB GP)
0.15
0.10
0.05
0.00
-0.05
-0.10
0
100
200
300
400
500
600
700
800
900
1000
Time (Seconds)
Initial Hydrolysis
Hydrolysis after 1 hour incubation in serum-less medium

Figure 12

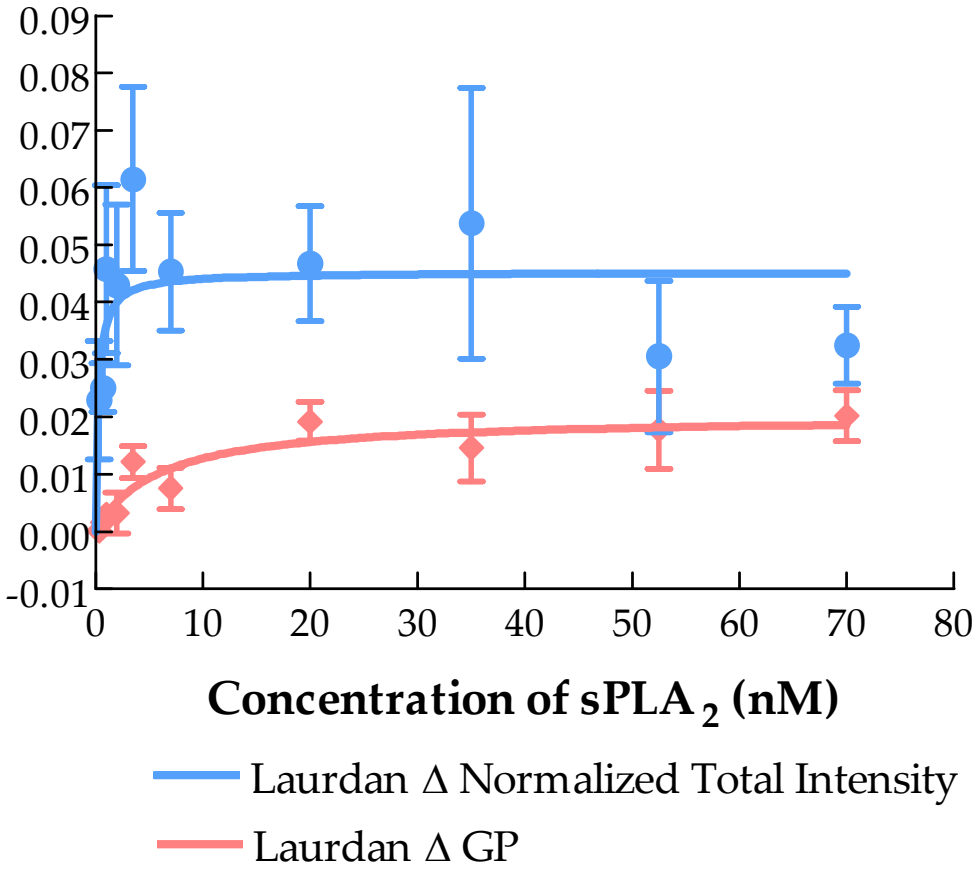
0.09
0.08
0.07
0.06
0.05
0.04
0.03
0.02
0.01
0.00
-0.01
0
10
20
30
40
50
60
70
80
Concentration of sPLA 2 (nM)
Laurdan Δ Normalized Total Intensity
Laurdan Δ GP

Figure 13

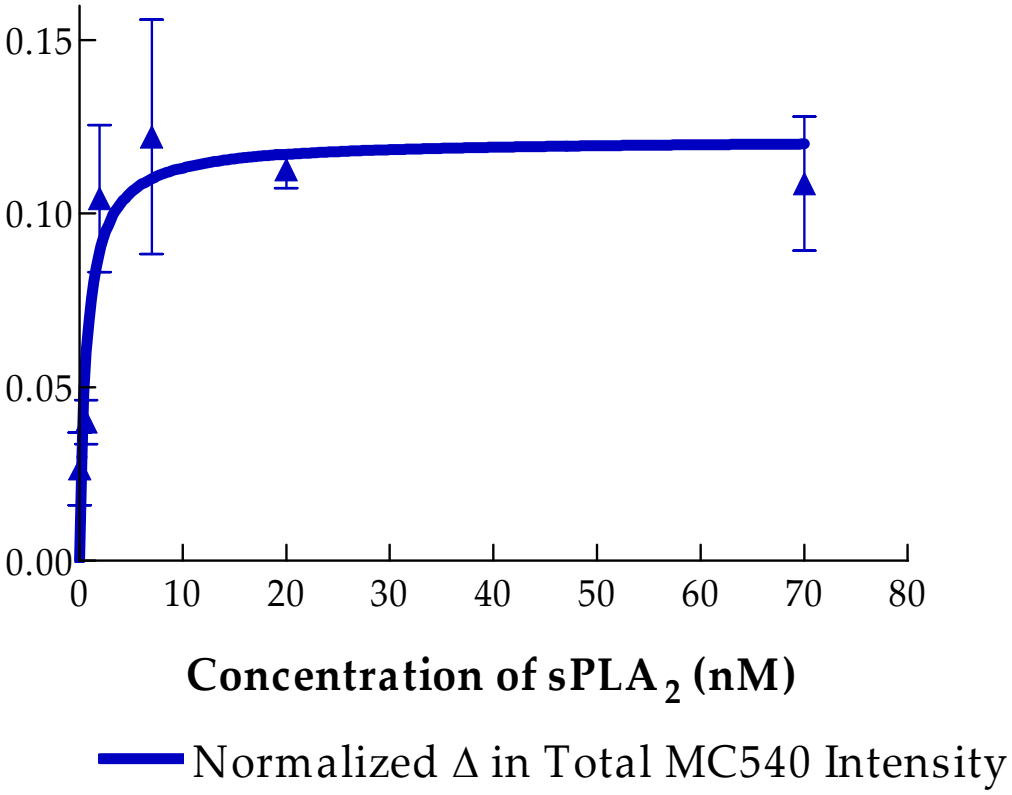
0.15
0.10
0.05
0.00
0
10
20
30
40
50
60
70
80
Concentration of sPLA2 (nM)
Normalized Δ in Total MC540 Intensity

Figure 14

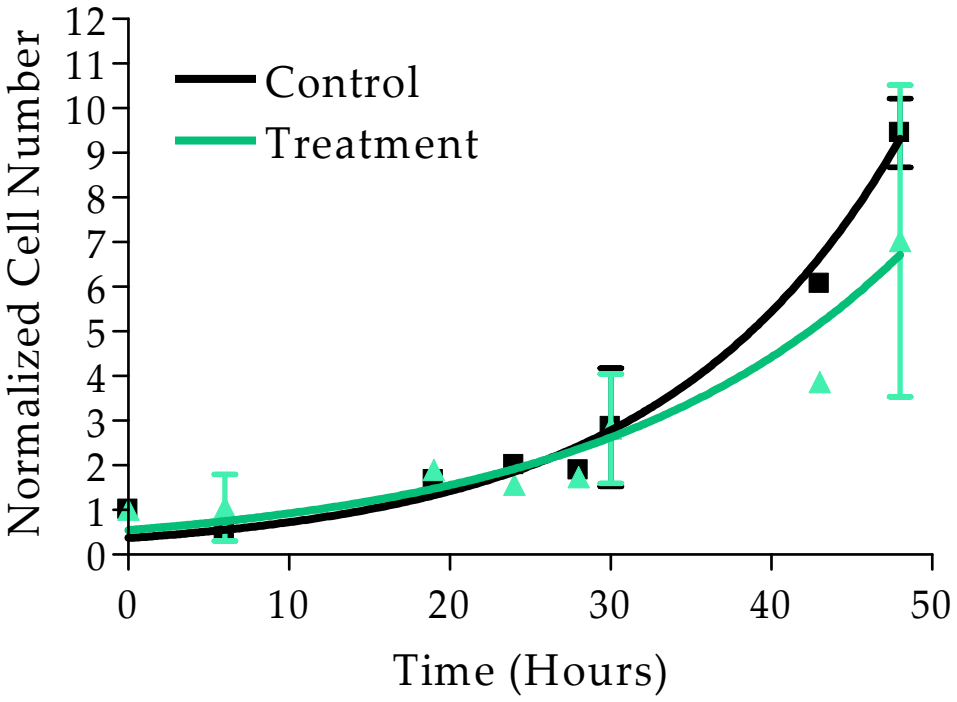
Normalized Cell Number
Control
Treatment
0
1
2
3
4
5
6
7
8
9
10
11
12
0
10
20
30
40
50
Time (Hours)

Figure 15

A

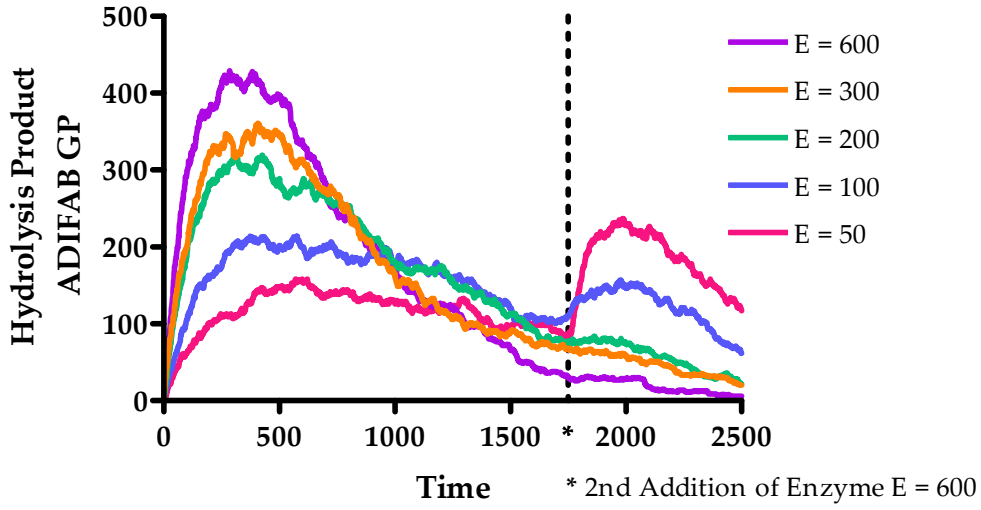
Hydrolysis Product
ADIFAB GP
500
400
300
200
100
0
0
500
1000
1500
*
2000
2500
Time
E = 600
E = 300
E = 200
E = 100
E = 50
* 2nd Addition of Enzyme E = 600

B

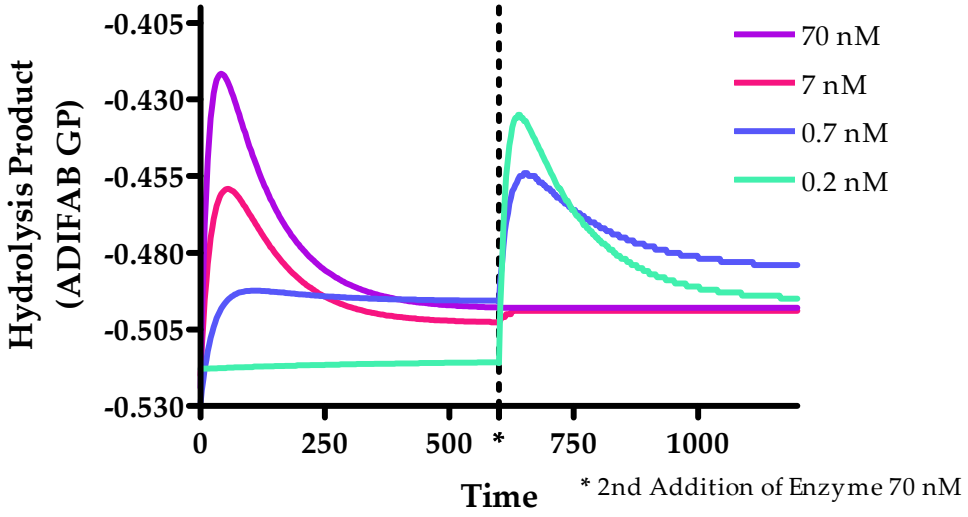
Hydrolysis Product
(ADIFAB GP)
-0.405
-0.430
-0.455
-0.480
-0.505
-0.530
0
250
500
*
750
1000
Time
70 nM
7 nM
0.7 nM
0.2 nM
* 2nd Addition of Enzyme 70 nM

Figure 16

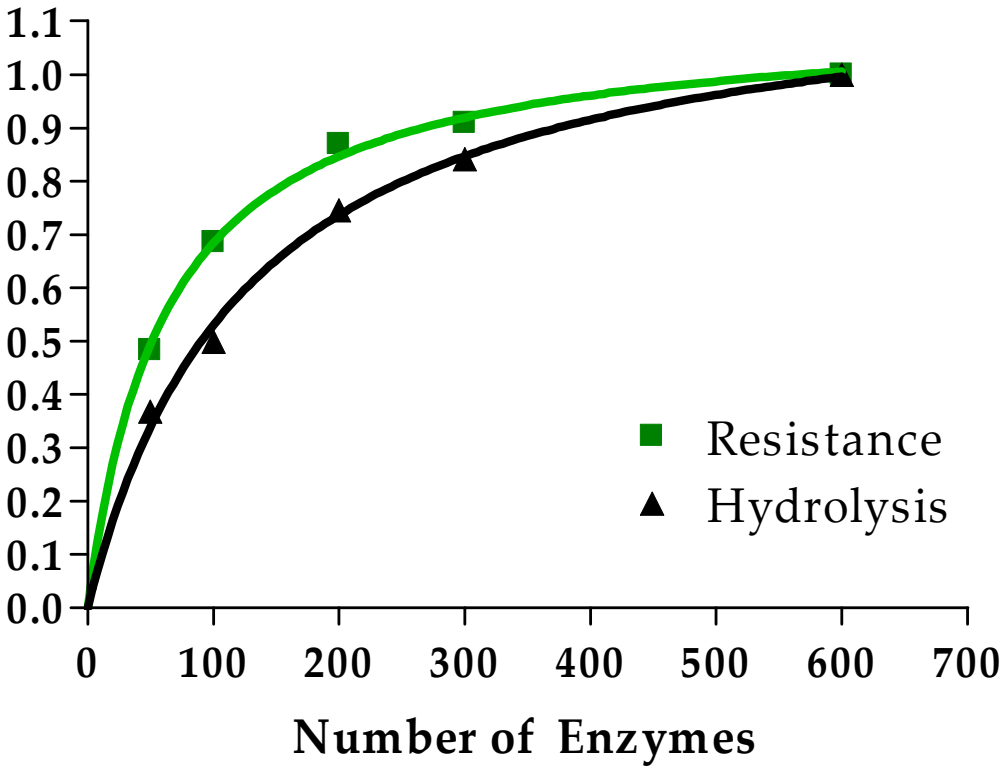
1.1
1.0
0.9
0.8
0.7
0.6
0.5
0.4
0.3
0.2
0.1
0.0
0
100
200
300
400
500
600
700
Number of Enzymes
Resistance
Hydrolysis

Jennifer Nelson

205 North 800 East Provo Ut 84606 801-372-8295 jennelson5@hotmail.com

Education

M.S. in Physiology & Developmental Biology

2006-2008 Brigham Young University Provo, UT

Thesis: Investigating and Modeling Mechanisms by which Healthy Cell Membranes Become Resistant to Secretory Phospholipase A2

B.S. in Biology

1999-2006 Brigham Young University Provo, UT

Emphasis: Human Physiology

Minor: Chemistry

Work & Teaching Experience

Research Assistant: Bell Lab

2006-2008 Brigham Young University Provo, UT

Emphasis: Interaction of secretory phospholipase A2 with cellular membranes

Skills acquired: Extensive use of programming in Microsoft Excel to analyze student performance and assessment validity

Research Assistant: Drs. Bradshaw and Bell

1999-2006 Brigham Young University Provo, UT

Emphasis: Dissemination of ideas concerning teaching students analytical thinking skills

Skills acquired: Extensive use of programming in Microsoft Excel to analyze student performance and assessment validity

Summer Research Fellow: National Institutes of Health

2006 Laboratory of Structural Biology, NIAMS Bethesda, MD

Emphasis: Three dimensional reconstruction of Hepatitis B capsid

Teaching Assistant: Cell Biology & Introductory Biology

2005-2006 Brigham Young University Provo, UT

The structure of these courses is unique in that it emphasizes analytical thinking as well as understand the subject material. Taught help sessions,

Research Assistant: Belnap Lab

1999-2006 Brigham Young University Provo, UT

Emphasis: Study of viral structure using cryo-electron microscopy

Skills acquired: Use of electron microscope, extraction of particle images, correction of particle images, use of pft2 and em3dr2 to make reconstructions, and use of pseudo-atomic modeling programs

Grants & Scholarships

Grant: Office of Research and Creative Activities
2005-2006 Brigham Young University Provo, UT

Funded proposal: A Study of Analytical Reasoning Skills: What are the cognitive dimensions? What BYU courses successfully promote them?

Scholarship: Heritage Scholar
1999-2004 Brigham Young University Provo, UT

100% Tuition Undergraduate Scholarship

Peer-Reviewed Articles

In progress: Publications with respect to Hepatitis B, secretory phospholipase A2, analytical thinking skills, and student mobility profile.

Oral Presentations & Research Abstracts

Biophysical Society 52nd Annual Meeting & International Biophysics Congress
February 2008

Nelson-Keller J, Yeung CH, LaFrance D, Bell JD, Judd AM
Abstract Title: Investigating and Modeling Possible Mechanisms by which Healthy Cell Membranes Become Resistant to Secretory Phospholipase A2

Bailey RW, Gibbons E, Robertson L, Nguyen T, Nelson J, Judd Am, Bell JD
Biophysical Changes in the Plasma Membrane during Glucocorticoid-stimulated Apoptosis Promote Hydrolysis by Secretory Phospholipase A2

Biophysical Society 52nd Annual Meeting & International Biophysics Congress
February 2008

Nelson-Keller J, Yeung CH, LaFrance D, Bell JD, Judd AM
Abstract Title: Investigating and Modeling Possible Mechanisms by which Healthy Cell Membranes Become Resistant to Secretory Phospholipase A2

American Society for Cell Biology Annual Meeting
December 2007

Bradshaw W, Keller J, Boren K, Bell JD
Abstract Title: Personal and Attitudinal Predictors of Performance on Analytical Reasoning Tasks in Cell Biology: Helping Students Improve Their Study Methods

American Society for Cell Biology Annual Meeting
December 2006

Bell JD, Bradshaw W, Nelson J
Abstract Title: The Student Mobility Profile: An Instrument for Measuring the Effectiveness Efforts to Improve Teaching and Learning

20th Annual Spring Research Conference

2006 Brigham Young University Provo, UT

Presentation Title: Multiple Conformations of the Hepatitis B Capsid: A Question of Handedness

Professional Membership

2007-2008 Biophysical Society

Service

Counsel Member: Graduate Student Society

2007-2008 Brigham Young University Provo, UT

Volunteer Representative: The Church of Jesus Christ of Latter-day Saints

2007-2008 Uruguay

Skills acquired: Effective communication, personalized teaching, detailed scheduling and planning